IEEE Access
Multidisciplinary ⋮ Rapid Review ⋮ Open Access Journal

Received 22 August 2023, accepted 28 October 2023, date of publication 6 November 2023, date of current version 9 November 2023.

Digital Object Identifier 10.1109/ACCESS.2023.3330167

RESEARCH ARTICLE

Numerical and Experimental Investigations on Robust Output Feedback Control for Active Vibration Attenuation of Flexible Smart System

ARUN P. PARAMESWARAN[1], ANJAN N. PADMASALI[1], AND K. V. GANGADHARAN[2]

[1]Department of Electrical and Electronics Engineering, Manipal Institute of Technology, Manipal Academy of Higher Education, Manipal, Udupi 576104, India
[2]Department of Mechanical Engineering, National Institute of Technology Karnataka (NITK), Surathkal, Mangalore 575025, India

Corresponding author: Anjan N. Padmasali (anjan.np@manipal.edu)

This work was supported in part by the SOLVE: The Virtual Laboratory, National Institute of Technology Karnataka (NITK) (http://rtlabs.nitk.ac.in/), through the Ministry of Human Resources Development, under Grant F.16-35/2009-DL; and in part by the Centre for System Design (CSD): A Centre of Excellence, NITK-Surathkal.

ABSTRACT This paper investigates the prototyping and implementation of an output feedback-based robust controller on a Field Programmable Gate Array (FPGA) platform. The Smart System under Test (SSuT) in this submission is a flexible cantilever beam bonded with Piezoelectric (PZT 5H) patches that act as a sensor as well as an actuator (perturbance creation as well as control actuation). For ease of modeling and subsequent controller design in the laboratory studies, the low-frequency dynamics of the smart system are approximated to only a Single Degree of Freedom (SDOF) in terms of flexural vibrations. The SSuT is modeled analytically through finite element modeling and experimentally through sub-space system identification process. The developed models' accuracy is compared with the experimental results of non - parametric modeling. The developed models are then used to conduct the simulation studies with the designed robust output feedback controller in the closed loop. Apart from the simulation studies, the designed controller was also prototyped on an FPGA platform using LabVIEW FPGA with the associated hardware in loop to carry out the experimental validation of its performance. The robustness and efficiency of the prototype controller to control the system vibrations in real-time were proved through extensive tests at single resonant frequencies and a range of frequencies encompassing the dominant resonant regions in the flexural mode. Findings from this study are further used to ensure satisfactory active vibration control of smart cantilever systems in various heavy/aerospace industries by approximating them to suitable benchmark systems in the laboratory.

INDEX TERMS Smart systems, active vibration control, mathematical modeling, LabVIEW FPGA, output feedback control, simulation and real-time control.

I. INTRODUCTION

Low-frequency dynamics of an electro-mechanical system can be best analyzed via the occurring vibrations. These vibrations tend to affect the stability as well as operational efficiency of real-time systems/machines/structures, especially at the dominant resonant frequencies [1], [2]. Hence, Active Vibration Control (AVC) at these low frequencies is of great importance as it ensures the stability as well as the subsequent precise operational ability of real-time systems of various scales [3], [4], [5], [6], [7]. The simplest and most effective method of actively controlling the system vibrations is via direct output feedback-based proportional control with the measured parameter being strain, displacement, acceleration, velocity, etc., as studied and proved by [8], [9], [10], [11], [12], [13], and [14]. Active vibration control of cantilever beam structures is also achieved using hybrid feedback PID-FxLMS algorithm, which combines

The associate editor coordinating the review of this manuscript and approving it for publication was Shunfeng Cheng.

the feedback FxLMS algorithm and conventional PID controller [15]. Modern optimal controllers like Linear Quadratic Regulator (LQR), Linear Quadratic Gaussian (LQG), and H-infinity [16] are implemented in experimental investigations for active vibration control of cantilever beams. Simulation and experimental studies have highlighted the independent modal space optimal control techniques based on LQR [17] for the active control of the smart beam structure incorporating uncertainties. Fractional order model reference adaptive controllers have also been explored to achieve active vibration isolation of piezo actuated systems [18]. Accelerometers [13], [19], [20], [21], [22], strain gauges [23], [24], laser doppler vibrometers [25], [26], [27], [28], [29] and embedded piezoelectric patches [8], [9], [10], [30], [31], [32], [33], [34] are some of the transducers used to measure the system vibrations for subsequent design and realization of active vibration controllers. Piezoelectric transducers/actuators are highly popular in achieving active vibration control, especially at low frequencies of flexible systems/structures [35]. This is attributed to its various inherent features such as light in weight, embedding of the transducer/actuator onto the system/structure via suitable adhesive, low power consumption, high force output, quick response time, as well as the absence of magnetic field and its associated effects during the electromechanical energy conversion process [36]. Any system vibration control is possible only by first capturing the system's dynamics on a simulation platform [37]. The authors in their work [38] highlighted the finite element modeling procedure used to model their system under study mathematically. By implementing displacement and velocity feedback control strategies, active control of the system vibrations was achieved. The authors in their work [10], [30], [31], [33], [34], [39], [40] developed analytical models of the piezo-composite cantilever beam employing finite element techniques incorporating the dynamics of the beam as well as piezo patch elements. Further, through successful simulations as well as in real-time, prototypes of classical [10], [33] and robust active controllers [30], [31], [34] were developed and deployed in the loop for control of system vibrations. An experimental study on active vibration damping of a cantilever structure was undertaken by [41], wherein the system was modeled via system identification technique with a state feedback controller designed by pole placement method operating in the closed loop.

II. SYSTEM DESCRIPTION AND METHODOLOGY

In the submitted work, the non-parametric modeling of the SuT was theoretically determined and further validated experimentally [8], [9], [10]. The obtained results from the non-parametric modeling process are shown in Table 1. Subsequently, the parametric model was derived [10], [30], [31], [37]. Further, from the experimentally obtained input output data of the SuT, sub-space-based system identification techniques [42], [43], [44] were implemented to identify

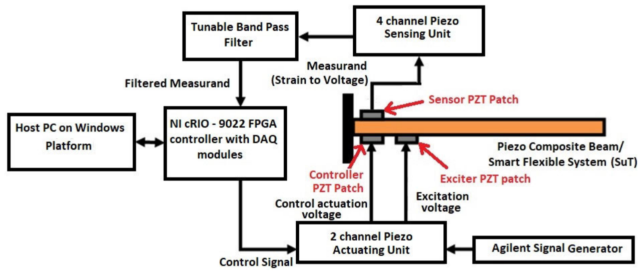

FIGURE 1. Block schematic of Active Vibration Control of SSuT with Hardware in loop.

its accurate mathematical model. This yielded a highly accurate open-loop model incorporating the piezo exciter-sensor dynamics. The frequency responses of the identified mathematical models validated the results obtained in the non-parametric modeling procedure. An impulse test was carried out on the system [10], [30], [31]. Figure 1 depicts the complete active vibration control of the SSuT with the embedded hardware in loop employed in this study. The host-PC is used to visualise the results of the controllers operation as well as to input the changes required in the controller parameters without halting its execution. The dominant flexural modes of vibrations were recorded from the spectral response shown in Fig. 2. The corresponding piezo sensor voltages were recorded as in Table 2, from which the dominant flexural modes (SDOF dynamics in focus) were determined to exist only till the second flexural mode. Accordingly, the scope of this work was restricted to the first two dominant modes of flexural vibrations of the SuT. In the final stage, a novel robust output feedback-based controller was designed and tested through computer simulations. The controller efficiency was tested at individual resonant frequencies and over a range that included the dominant resonant frequencies. Subsequently, the designed controller was prototyped on an FPGA platform using LabVIEW FPGA with the associated hardware in loop. Its operational efficiency was validated through the same individual and multi-mode resonant conditions. Thus, real-time active control of vibrations of the SSuT was achieved through this novel controller, which is an essential contribution to the existing literature in the same field. The understanding from the results presented here forms

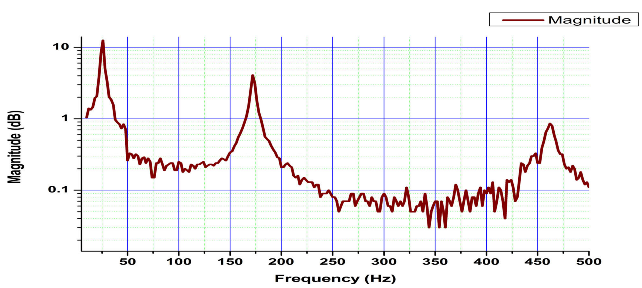

FIGURE 2. Spectral response of SuT to impulse test.

TABLE 1. Parameters of System under Test (SuT) - Aluminum cantilever beam with embedded piezoelectric patches.

Quantity	Symbol	Value
Beam length	L_b	0.3m
Beam Width	b	0.025m
Beam Thickness	h	0.003m
Young's Modulus	E_b	$70GPa$
Beam Density	ρ_b	$2700kg/m^3$
First Natural Frequency	f_{n_1}	27.05 Hz
Beam Stiffness	K	$443.75N/m$
Damping coefficient	c	$0.07203Ns/m$
Actuator length	L_p	0.05m
Actuator width	b_p	0.025m
Actuator thickness	H_p	0.0005m
Actuator density	ρ_p	$7700kg/m^3$
Young's Modulus of actuator	E_p	$68GPa$
PZT strain constant	d_{31}	$125 \times 10^{-12} m/V$
PZT stress constant	g_{31}	$10.5 \times 10^{-13} V-m/N$

TABLE 2. Measured flexural modes and related piezo sensor voltage.

Measurand	Symbol	Voltage (V_{rms})
First Natural Frequency	$f_{n_1} = 27.05Hz$	3.95V
Second Natural Frequency	$f_{n_2} = 172.53Hz$	1.05V
Fourth Natural Frequency	$f_{n_4} = 462.23Hz$	0.62V

the basis of developing and prototyping further advanced controllers covering multiple degrees of freedom, which can then be extrapolated to actual cantilever systems in various heavy/aerospace industries.

III. ANALYTIC APPROACH TO MODELING OF THE SSuT

The low-frequency dynamics of a flexible beam element is determined by the fourth order partial differential equation shown in (1) as illustrated in work of [37], which was later applied in finite element modeling for deriving the global mass and global stiffness matrices of a piezoelectric laminate cantilever beam at first resonance by [10]. The system model derived here was also further used in the works of [30] and [31] to design various other robust active control strategies for damping the system vibrations.

$$E_b I_b \frac{\partial^4 w(x,t)}{\partial x^4} + \rho_b A_b \frac{\partial^2 w(x,t)}{\partial t^2} = f_{ext}{}^* \tag{1}$$

where E_b is the young's modulus of aluminum that constituted the beam element, A_b being the cross sectional area of the beam element, I_b being the moment of inertia calculated based on the geometry of the system, $w(x,t)$ is the displacement function of a two node beam element while $f_{ext}{}^*$ is the external force applied on the beam element. Now, through the application of suitable boundary conditions [10], [30], [31], [33], [34] the general solution to the low frequency dynamics of a two node beam element is determined as in (2)

$$w(x,t) = \frac{1}{L_b^3}\begin{pmatrix} L_b^3 & 0 & 0 & 0 \\ 0 & L_b^3 x & 0 & 0 \\ -3L_b x^2 & -2L_b^2 x^2 & 3L_b x^2 & -L_b^2 x^2 \\ 2x^3 & L_b x^3 & -2x^3 & L_b x^3 \end{pmatrix}\begin{pmatrix} w_1 \\ \theta_1 \\ w_2 \\ \theta_2 \end{pmatrix} \tag{2}$$

As shown in [30], [31], [33], and [34], the residual function (R_d) defined in (3) is solved as in (4) using a derived shape function q over the entire beam element length L_b from (2) so as to obtain the optimum solution.

$$R_d = E_b I_b \frac{\partial^4 w(x,t)}{\partial x^4} + \rho_b A_b \frac{\partial^2 w(x,t)}{\partial t^2} - f_{ext} \tag{3}$$

$$\int_0^{L_b} (R_d \times q) dx = 0 \tag{4}$$

Further analysis involved the beam element's mass M^b, stiffness K^b and it being subjected to a harmonic excitation with f_b being the force vector as in (5). This resulted in the optimum solution for motion of the beam element as derived in (6):

$$M^b \ddot{q} + K^b q = f^b(t) \tag{5}$$

$$\frac{\rho_b A_b L_b}{420}\begin{pmatrix} 156 & 22L_b & 54 & -13L_b \\ 22L_b & 4L_b^2 & 13L_b & -3L_b^2 \\ 54 & 13L_b & 156 & -22L_b \\ -13L_b & -3L_b{}^2 & -22L_b & 4L_b{}^2 \end{pmatrix}\begin{pmatrix} \ddot{w_1} \\ \ddot{\theta_1} \\ \ddot{w_2} \\ \ddot{\theta_2} \end{pmatrix} + \frac{E_b I_b}{L_b}\begin{pmatrix} \frac{12}{L_b^2} & \frac{6}{L_b} & \frac{-12}{L_b^2} & \frac{6}{L_b} \\ \frac{6}{L_b} & 4 & \frac{-6}{L_b} & 2 \\ \frac{-12}{L_b^2} & \frac{-6}{L_b} & \frac{12}{L_b^2} & \frac{-6}{L_b} \\ \frac{6}{L_b} & 2 & \frac{-6}{L_b} & 4 \end{pmatrix}\begin{pmatrix} w_1 \\ \theta_1 \\ w_2 \\ \theta_2 \end{pmatrix} = \begin{pmatrix} F_1 \\ -M_1 \\ -F_2 \\ M_2 \end{pmatrix} \tag{6}$$

Following the works of [37], the final state space model of the smart system derived through analytic means by analysing and solving (6) as shown in (7) and (8):

$$\begin{pmatrix} \dot{x_1} \\ \dot{x_2} \\ \dot{x_3} \\ \dot{x_4} \end{pmatrix} = \begin{pmatrix} 0 & I \\ -M^{*-1}K^* & -M^{*-1}C^* \end{pmatrix}\begin{pmatrix} x_1 \\ x_2 \\ x_3 \\ x_4 \end{pmatrix}$$

TABLE 3. Frequency comparison between analytic model and the physical system.

Natural Frequency	Analytical Model	Physical System
f_{n_1}	30.554 Hz	27.05 Hz
f_{n_2}	174.8684 Hz	172.53 Hz
f_{n_4}	472.4 Hz	462.23 Hz

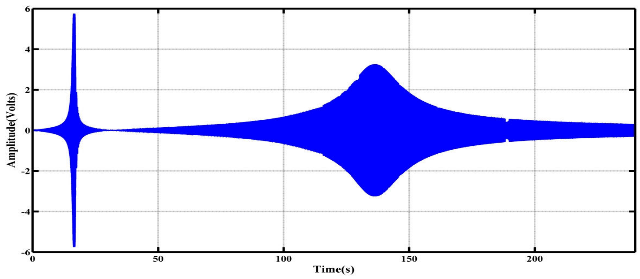

FIGURE 3. Time response of the developed model to sweep sine excitation for first two flexural modes.

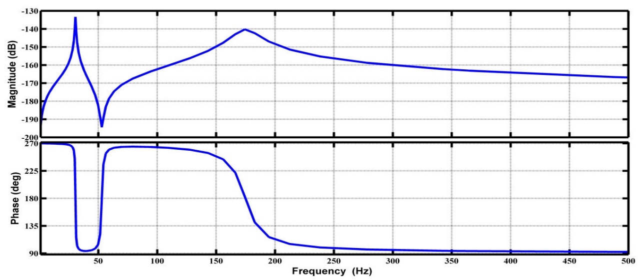

FIGURE 4. Frequency response of the developed model for first two flexural modes.

$$+\begin{pmatrix}0\\ {M^*}^{-1}T^T h\end{pmatrix}u(t)+\begin{pmatrix}0\\ {M^*}^{-1}T^T f\end{pmatrix}r(t) \quad (7)$$

$$y(t)=\begin{pmatrix}0 & p^T T\end{pmatrix}\begin{pmatrix}x_1\\ x_2\\ x_3\\ x_4\end{pmatrix} \quad (8)$$

Through analytic means, the mathematical models of the system corresponding to individual resonant frequencies and multiple modes of dominant resonance regions were derived. The bode plots of the derived models validated the accuracy of the entire modeling procedure in terms of a good match between the frequencies of the derived models with those of the physical system (observed from their nonparametric modeling). Table 3 highlights the close match between the resonant frequencies of the derived mathematical models with that of the real system for the first three dominant flexural resonances. The developed models were also subjected to sweep sine excitation covering the dominant frequency ranges as shown in Fig. 3. From the resulting frequency plot shown in Fig. 4, magnitude peaks were observed at the first and second resonance regions with the magnitude of the peak at second resonance considerably less than that at first resonance. This is in line with the understood theory of system vibrations as explained by [1] and [2].

IV. EXPERIMENTAL APPROACH TO MODELING OF SSuT

As shown by [45], a system identification technique can be adopted to estimate the properties of the SSuT and its dynamic response. Various excitation signals like step input [6], white noise [46], [47], and harmonic sweep sine excitation [10], [30], [31], [48], [49] can be used as the system input.

Reference [47] performed system identification after exciting a piezoelectric laminated plate by band-limited white noise excitation. From the measured data, a 3 × 3 reduced order multi-input, multi-output model was identified through the subspace identification method. With an impulse input [50], system identification techniques were employed to identify the mathematical models of an aluminium beam with piezoelectric sensing and actuation abilities for necessary AVC. The system models identified in this work are followed by the works of [30], [43], and [44]. The smart system was subjected to impulse and sweep sine excitation in an open loop. A second order analog bandpass filter was employed to minimize errors caused by system noises. From the measured input-output data, the input and output Block Hankel matrices were defined as in (9) and (10), respectively, with the subscripts p and f denoting the past and future instances.

$$U_{0|2i-1} \stackrel{def}{=} \left(\begin{array}{ccccc} u_0 & u_1 & u_2 & \cdots & u_{j-1}\\ u_1 & u_2 & u_3 & \cdots & u_j\\ \vdots & \vdots & \vdots & \vdots & \vdots\\ u_{i-1} & u_i & u_{i+1} & \cdots & u_{i+j-2}\\ \hline u_i & u_{i+1} & u_{i+2} & \cdots & u_{i+2}\\ u_{i+1} & u_{i+2} & u_{i+3} & \cdots & u_{i+j-1}\\ \vdots & \vdots & \vdots & \vdots & \vdots\\ u_{2i-1} & u_{2i} & u_{2i+1} & \cdots & u_{2i+j-2} \end{array}\right) \stackrel{def}{=} \begin{pmatrix}U_{0|i-1}\\ \hline U_{i|2i-1}\end{pmatrix} \stackrel{def}{=} \begin{pmatrix}U_p\\ U_f\end{pmatrix} \quad (9)$$

$$Y_{0|2i-1} \stackrel{def}{=} \begin{pmatrix}Y_p\\ Y_f\end{pmatrix} \quad (10)$$

As shown in (11), the projection matrix (Z_i) can be computed from the measured data (Past inputs and outputs W_p and future system input U_f) without the knowledge of future system outputs (Y_f).

$$Z_i = Y_f / \begin{pmatrix}W_p\\ U_f\end{pmatrix} = \Gamma_i \hat{X}_i + H_i^d U_f \quad (11)$$

where, the Kalman filter state sequence ($\hat{X}_i$) is defined in terms of the initial state matrix ($\hat{X}_0$) as well as initial matrix (P_0) as $\hat{X}_i \stackrel{def}{=} \hat{X}_{i[\hat{X}_0,P_0]}$ With $W_1 \in \Re^{li \times li}$ and $W_2 \in \Re^{j \times j}$ being user defined weighting matrices, the extended observability matrix can be written as in (12)

$$\Gamma_i = W_1^{-1} U_1 S_1^{1/2} T \quad (12)$$

The projection matrix can be written as in (13)

$$Z_{i+1} = Y_f^- / \begin{pmatrix} W_p^+ \\ U_f^- \end{pmatrix} = \Gamma_{i-1}\hat{X_{i+1}} + H_{i-1}^d U_f^- \tag{13}$$

with $\hat{X_{i+1}} \stackrel{def}{=} \hat{X}_{i+1[\hat{X}_0, P_0]}$. $(W_p^+, U_f^- and Y_f^-)$ are the reorganized matrices obtained from the measured input - output data. Further solution results in the representation of the system matrices in terms of the Kalman filter estimates at instants $'i'$ and $'i+1'$ are obtained as shown in (14)

$$\begin{pmatrix} \hat{X_{i+1}} \\ y_{i|i} \end{pmatrix} = \begin{pmatrix} A & B \\ C & D \end{pmatrix} \begin{pmatrix} \hat{X}_i \\ U_{i|i} \end{pmatrix} + \begin{pmatrix} \rho_w \\ \rho_v \end{pmatrix} \tag{14}$$

where ρ_w and ρ_v are the residuals from which the covariances are computed. Sub-space-based system identification techniques identified the vibrating system's mathematical models for the first two and first three flexural modes, just as was done in analytical modeling. The procedure was repeated in the experimental tests by subjecting the system to harmonic excitations of varying frequencies covering the first two flexural modes. Fig. 5 illustrates the close match between the dynamics of the identified model with that of the actual system, thereby validating the identified model of the system under test for the first two flexural modes of vibrations.

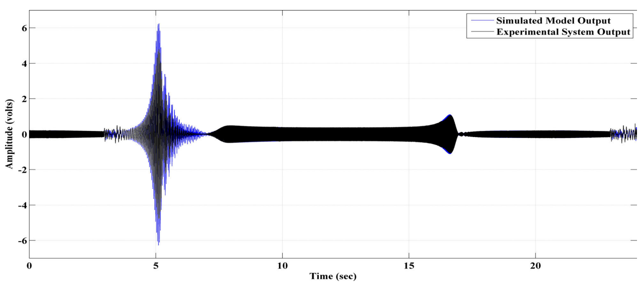

FIGURE 5. Comparison of the sweep sine responses of the system and its identified model for first two flexural modes.

V. DESIGN OF THE OUTPUT FEEDBACK ROBUST CONTROLLER FOR ACTIVE CONTROL OF VIBRATIONS OF SSuT

In this manuscript, active control of the vibrations occurring in the piezo composite beam was controlled via the output feedback-based control strategy. The controller was designed from the fundamental principles as discussed in [51]. The efficiency of the designed controller was tested and validated in the simulations studies. After that, the controller was prototyped using the cRIO FPGA controller using the LabVIEW FPGA software platform. An n^{th} order system is described in (15) as:

$$\begin{aligned} \dot{x} &= Ax + Bu \\ y &= Cx \end{aligned} \tag{15}$$

The control law is selected as in (16)

$$u = -K\hat{x} + K_r r \tag{16}$$

where the n^{th} order observer output $(\hat{x})$ is expressed as:

$$\dot{\hat{x}} = A\hat{x} + Bu + L(y - C\hat{x}) \tag{17}$$

Appropriate analysis of the closed loop system was achieved by replacing $\hat{x}$ by:

$$\tilde{x} = x - \hat{x} \tag{18}$$

Subsequent calculations yielded (19)

$$\dot{\tilde{x}} = (A - LC)\tilde{x} \tag{19}$$

Introducing (16) and (18) in (19) and upon further simplification resulted in (20)

$$\dot{x} = (A - BK)x + BK\tilde{x} + BK_r r \tag{20}$$

Hence, the final state equation of the closed loop system can be written as:

$$\begin{pmatrix} \dot{x} \\ \dot{\tilde{x}} \end{pmatrix} = \begin{pmatrix} A - BK & BK \\ 0 & A - LC \end{pmatrix} \begin{pmatrix} x \\ \tilde{x} \end{pmatrix} + \begin{pmatrix} BK_r \\ 0 \end{pmatrix} r \tag{21}$$

In the first stage of the simulations, the system was subjected to harmonic excitation at its first resonant frequency of 27.05 Hz. The introduction of the controller in the loop resulted in a substantial reduction of the system vibrations, as shown in Table 4. Subsequently, the system was excited at the next dominant resonant frequency of 172.53 Hz, and the controller effectively damped out the sensed vibrations at the second resonance. The robustness of the output feedback controller was verified from the sweep sine excitation, which was conducted for multiple modes of flexural vibrations covering the dominant resonant frequencies. Fig 6 and Fig 7 depict the vibrating system's open loop and closed loop responses when subjected to sweep sine excitation covering the first two dominant resonant regions.

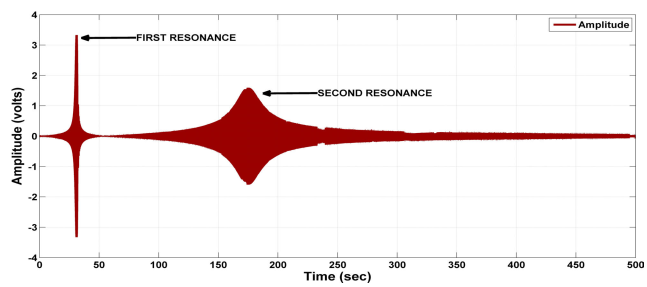

FIGURE 6. Open loop piezo sensor voltage waveform to sweep sine excitation for first two flexural modes of vibrations.

VI. EXPERIMENTAL VALIDATION OF ACTIVE CONTROL OF VIBRATIONS OF THE SSuT WITH THE FPGA CONTROLLER IN LOOP

In the final section, the designed controller was implemented in real-time on a Field Programmable Gate Array (FPGA) platform using the LabVIEW FPGA software platform with the necessary hardware in the loop. The controller was prototyped using LabVIEW FPGA and transferred via the Local Area Network to the remote Compact Reconfigurable

TABLE 4. Performance evaluation (Simulations) of the designed controller over various modes of system excitation.

Mode of Excitation	Frequency	Exciter voltage	Control voltage	Sensor voltage (open loop)	Sensor voltage (closed loop)	% reduction in vibrations
First Resonance	27.05 Hz	$160V_{p-p}$	$240V_{\mathrm{p-p}}$	$5.2V_{p-p}$	$1.6V_{p-p}$	70%
Second Resonance	172.53 Hz	$160V_{p-p}$	$120V_{p-p}$	$2.3V_{p-p}$	$0.53V_{p-p}$	88.5%
First Two Flexural Modes	5-200 Hz	$353.5V_{p-p}$	$380V_{p-p}$ at 1^{st} resonance $250V_{p-p}$ at 2^{nd} resonance	$6.4V_{p-p}$ at 1^{st} resonance $3.2V_{p-p}$ at 2^{nd} resonance	$1.1V_{p-p}$ at 1^{st} resonance $0.76V_{p-p}$ at 2^{nd} resonance	82.8% at 1^{st} resonance 76.3% at 2^{nd} resonance

TABLE 5. Real time performance evaluation of the prototyped FPGA controller over various modes of system excitation.

Mode of Excitation	Frequency	Exciter voltage	Control actuator voltage	Sensor voltage (open loop)	Sensor voltage (closed loop)	% reduction in vibrations
First Resonance	27.05 Hz	$120V_{\mathrm{p-p}}$	$110V_{p-p}$	$14V_{p-p}$	$3V_{p-p}$	78.57%
Second Resonance	172.53 Hz	$80V_{p-p}$	$60V_{p-p}$	$3.3V_{p-p}$	$0.8V_{p-p}$	75.75%
First Two Flexural Modes	5-200 Hz			$21V_{p-p}$ at 1^{st} resonance $5.2V_{p-p}$ at 2^{nd} resonance	$4.8V_{p-p}$ at 1^{st} resonance $0.9V_{p-p}$ at 2^{nd} resonance	77.14% at 1^{st} resonance 82.69% at 2^{nd} resonance

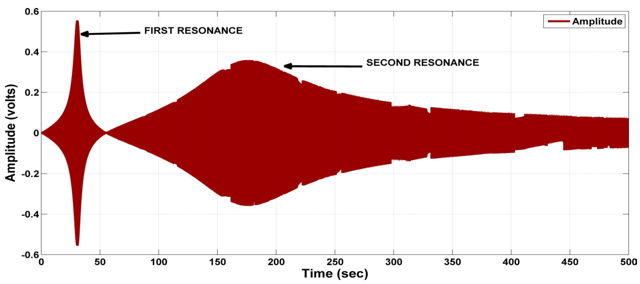

FIGURE 7. Piezo sensor voltage waveform to sweep sine excitation for first two flexural modes of vibrations in closed loop.

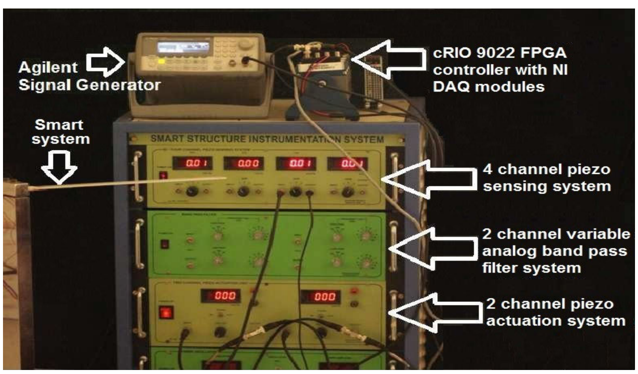

FIGURE 8. Experimental setup with hardware in loop.

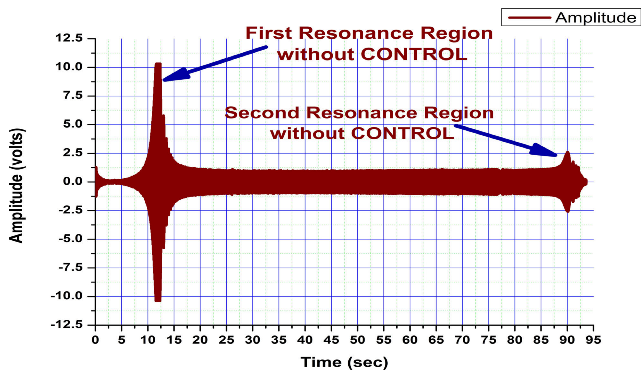

FIGURE 9. Open loop sweep sine sensor voltage waveform for the first two flexural modes of vibrations.

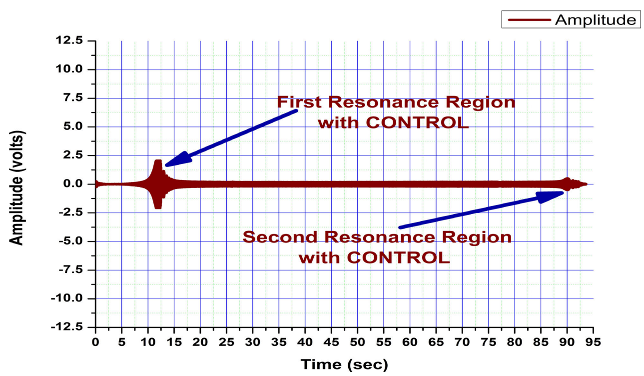

FIGURE 10. Closed loop sweep sine sensor voltage waveform for the first two modes of vibrations.

Input Output (cRIO-9022) controller, which was connected to the piezo sensor/ actuator amplifier systems. The block schematic of the closed-loop system with the FPGA controller in the loop is shown in Fig 1. The pictorial view of the experimental setup used in this study is shown in Fig 8. Apart from testing the controller's efficiency at individual resonant frequencies in real-time, as in simulation studies, the closed-loop system was subjected to sweep sine excitation covering multiple modes of dominant flexural vibrations. Table 5 along with Fig 9 and Fig 10 depict the experimental

TABLE 6. Comparison of control efficiency of the proposed outpit feedback controller with other FPGA controllers on the same SSuT.

Sl No.	Type of FPGA Controller	Control performance at first resonance	Control performance at second resonance
1	Proportional (P) controller [9], [10]	60.80%	-
2	Proportional Integral (PI) controller [9], [10]	63.00%	-
3	Proportional Integral Derivative (PID) controller [9], [10]	61.60%	-
4	Pole Placement State Feedback (PPSF) controller [34]	63.40%	25.40%
5	Proportional Derivative Sliding Mode (PDSM) controller [30], [31]	85.48%	82.64%
6	**Proposed Output Feedback (OF) controller**	**78.57%**	**75.75%**

results of harmonic as well as sweep sine excitation of the closed loop system, thereby confirming satisfactory active control of the smart system at the dominant regions of vibrations.

VII. DISCUSSION AND CONCLUSION

The work presented in this manuscript showcases an elaborate study of mathematical modeling through analytical and experimental means of a vibrating piezoelectric laminate cantilever beam (smart system) for individual and multiple modes of flexural vibrations. The mathematical model developed through both techniques is analyzed in both - time and frequency domains and the obtained results validate the entire modeling procedure adopted in this study. The proposed controller's performance is compared with other FPGA controllers deployed for the same intelligent system with the same hardware in loop conditions. The results of the control performance of the implemented FPGA controllers for dominant resonant regions are depicted in table 6. It is observed that the computational complexity, as well as memory resources needed for the execution of the proposed controller, is less, and its control performance is comparable with that of the listed FPGA controllers. As the table shows, the proposed Output Feedback (OF) controller's performance is highly satisfactory from a real-time execution perspective. Consequently, with further tuning of the controller parameters, its operational performance can exceed that of the implemented PDSM controller. The distinct features of this paper are summarized as follows:

1) Application of the core mathematical principle named combined deterministic – stochastic subspace-based system identification for developing a highly accurate mathematical model of a time-invariant low-frequency dynamics of an intelligent benchmark engineering system.
2) The proposed and implemented robust controller takes very little computational time and memory resources. This is a highly desirable feature of real-time active vibration control for applications with fast-time invariant dynamics in heavy industries, aerospace, etc.
3) The proposed robust controller has been tested in simulations and experimentally verified for an Euler-Bernoulli smart cantilever beam, whose vibrations are more profound, especially during low-frequency resonance. This is an update to the existing literature, where a similar controller was implemented for a smart Timoshenko cantilever beam [39], [40]
4) The conducted experimental investigation involved an FPGA platform, due to which the controller parameters could be varied in real-time in the loop without halting its execution. This feature makes it attractive for developing a practical Application-Specific Integrated Circuit (ASIC).

The simulation studies illustrated the efficiency of the designed output feedback controller at individual modes and the multiple modes of flexural vibrations, which are dominant in vibrations-related voltage amplitude. The operational efficiency of the controller was validated in real-time by prototyping it on a low-level FPGA platform using LabVIEW FPGA coupled with the necessary DAQ hardware and cRIO controller configured in its FPGA interface mode. From the experimental studies, the developed controller was found to be highly satisfactory in controlling the major modes of vibrations, which usually threaten the stability and operational efficiency of the smart system.

REFERENCES

[1] S. S. Rao and F. F. Yap, *Mechanical Vibrations*, vol. 4. New York, NY, USA: Addison-Wesley, 1995.
[2] W. Thomson, *Theory of Vibration With Applications*. Boca Raton, FL, USA: CRC Press, 1996.
[3] M. Grossard, M. Boukallel, N. Chaillet, and C. Rotinat-Libersa, ''Modeling and robust control strategy for a control-optimized piezoelectric microgripper,'' *IEEE/ASME Trans. Mechatronics*, vol. 16, no. 4, pp. 674–683, Aug. 2011.
[4] T. Knüppel, J. N. Nielsen, K. H. Jensen, A. Dixon, and J. Østergaard, ''Power oscillation damping capabilities of wind power plant with full converter wind turbines considering its distributed and modular characteristics,'' *IET Renewable Power Gener.*, vol. 7, no. 5, pp. 431–442, 2013.
[5] G.-Y. Gu, L.-M. Zhu, C.-Y. Su, and H. Ding, ''Motion control of piezoelectric positioning stages: Modeling, controller design, and experimental evaluation,'' *IEEE/ASME Trans. Mechatronics*, vol. 18, no. 5, pp. 1459–1471, Oct. 2013.
[6] M. Rakotondrabe, I. A. Ivan, S. Khadraoui, P. Lutz, and N. Chaillet, ''Simultaneous displacement/force self-sensing in piezoelectric actuators and applications to robust control,'' *IEEE/ASME Trans. Mechatronics*, vol. 20, no. 2, pp. 519–531, Apr. 2015.
[7] E. Eshraqi, M. Shahravi, and M. Azimi, ''Consideration of spillover effect in active vibration suppression of a smart composite plate using piezoelectric elements,'' *Latin Amer. J. Solids Struct.*, vol. 13, no. 14, pp. 2643–2656, 2016.
[8] A. P. Parameswaran and K. V. Gangadharan, ''Active vibration control of a smart cantilever beam at resonance: A comparison between conventional and real time control,'' in *Proc. 12th Int. Conf. Intell. Syst. Design Appl. (ISDA)*, Nov. 2012, pp. 235–239.
[9] A. Parameswaran, A. Pai, P. Tripathi, and K. Gangadharan, ''Active vibration control of a smart cantilever beam on general purpose operating system,'' *Defence Sci. J.*, vol. 63, no. 4, pp. 413–417, Jul. 2013.

[10] A. P. Parameswaran and K. Gangadharan, "Parametric modeling and FPGA based real time active vibration control of a piezoelectric laminate cantilever beam at resonance," *J. Vibrat. Control*, vol. 21, no. 14, pp. 2881–2895, Oct. 2015.
[11] F.-M. Li, K. Kishimoto, Y.-S. Wang, Z.-B. Chen, and W.-H. Huang, "Vibration control of beams with active constrained layer damping," *Smart Mater. Struct.*, vol. 17, no. 6, 2008, Art. no. 065036.
[12] F.-M. Li, Z.-G. Song, and Z.-B. Chen, "Active vibration control of conical shells using piezoelectric materials," *J. Vibrat. Control*, vol. 18, no. 14, pp. 2234–2256, Dec. 2012.
[13] S.-M. Kim and M. J. Brennan, "Active vibration control using delayed resonant feedback," *Smart Mater. Struct.*, vol. 22, no. 9, Sep. 2013, Art. no. 095013.
[14] M. M. Jovanović, A. M. Simonović, N. D. Zorić, N. S. Lukić, S. N. Stupar, and S. S. Ilić, "Experimental studies on active vibration control of a smart composite beam using a PID controller," *Smart Mater. Struct.*, vol. 22, no. 11, Nov. 2013, Art. no. 115038.
[15] W. Li, Z. Yang, K. Li, and W. Wang, "Hybrid feedback PID-FxLMS algorithm for active vibration control of cantilever beam with piezoelectric stack actuator," *J. Sound Vibrat.*, vol. 509, Sep. 2021, Art. no. 116243.
[16] S. M. Khot, N. P. Yelve, P. Kumar, G. A. Purohit, and D. Singh, "Experimental investigation of performances of different optimal controllers in active vibration control of a cantilever beam," *ISSS J. Micro Smart Syst.*, vol. 8, no. 2, pp. 101–111, Nov. 2019.
[17] M. Cui, H. Liu, H. Jiang, Y. Zheng, X. Wang, and W. Liu, "Active vibration optimal control of piezoelectric cantilever beam with uncertainties," *Meas. Control*, vol. 55, nos. 5–6, pp. 359–369, May 2022.
[18] S. Kang, H. Wu, X. Yang, Y. Li, and Y. Wang, "Fractional-order robust model reference adaptive control of piezo-actuated active vibration isolation systems using output feedback and multi-objective optimization algorithm," *J. Vibrat. Control*, vol. 26, nos. 1–2, pp. 19–35, Jan. 2020.
[19] H. Chen, M. Kurt, Y. S. Lee, D. M. McFarland, L. A. Bergman, and A. F. Vakakis, "Experimental system identification of the dynamics of a vibro-impact beam with a view towards structural health monitoring and damage detection," *Mech. Syst. Signal Process.*, vol. 46, no. 1, pp. 91–113, May 2014.
[20] K. Zhang, G. Scorletti, M. N. Ichchou, and F. Mieyeville, "Robust active vibration control of piezoelectric flexible structures using deterministic and probabilistic analysis," *J. Intell. Mater. Syst. Struct.*, vol. 25, no. 6, pp. 665–679, Apr. 2014.
[21] Z.-C. Qiu, H.-X. Wu, and C.-D. Ye, "Acceleration sensors based modal identification and active vibration control of flexible smart cantilever plate," *Aerosp. Sci. Technol.*, vol. 13, no. 6, pp. 277–290, Sep. 2009.
[22] C. Shin, C. Hong, and W. B. Jeong, "Active vibration control of beams using filtered-velocity feedback controllers with moment pair actuators," *J. Sound Vibrat.*, vol. 332, no. 12, pp. 2910–2922, Jun. 2013.
[23] A. J. Fleming and K. K. Leang, "Integrated strain and force feedback for high-performance control of piezoelectric actuators," *Sens. Actuators A, Phys.*, vol. 161, nos. 1–2, pp. 256–265, Jun. 2010.
[24] A. M. Simonovic, M. M. Jovanovic, N. S. Lukic, N. D. Zoric, S. N. Stupar, and S. S. Ilic, "Experimental studies on active vibration control of smart plate using a modified PID controller with optimal orientation of piezoelectric actuator," *J. Vibrat. Control*, vol. 22, no. 11, pp. 2619–2631, Jun. 2016.
[25] S. Leadenham and A. Erturk, "Unified nonlinear electroelastic dynamics of a bimorph piezoelectric cantilever for energy harvesting, sensing, and actuation," *Nonlinear Dyn.*, vol. 79, no. 3, pp. 1727–1743, Feb. 2015.
[26] Y. Wang and D. J. Inman, "Finite element analysis and experimental study on dynamic properties of a composite beam with viscoelastic damping," *J. Sound Vibrat.*, vol. 332, no. 23, pp. 6177–6191, Nov. 2013.
[27] T. Zhang and H. G. Li, "Adaptive pole placement control for vibration control of a smart cantilevered beam in thermal environment," *J. Vibrat. Control*, vol. 19, no. 10, pp. 1460–1470, Jul. 2013.
[28] T. Sangpet, S. Kuntanapreeda, and R. Schmidt, "Improving delay-margin of noncollocated vibration control of piezo-actuated flexible beams via a fractional-order controller," *Shock Vibrat.*, vol. 2014, pp. 1–8, Jan. 2014.
[29] M. S. Saad, H. Jamaluddin, and I. Z. M. Darus, "Active vibration control of a flexible beam using system identification and controller tuning by evolutionary algorithm," *J. Vibrat. Control*, vol. 21, no. 10, pp. 2027–2042, Jul. 2015.
[30] A. P. Parameswaran, B. Ananthakrishnan, and K. V. Gangadharan, "Modeling and design of field programmable gate array based real time robust controller for active control of vibrating smart system," *J. Sound Vibrat.*, vol. 345, pp. 18–33, Jun. 2015.
[31] A. P. Parameswaran, B. Ananthakrishnan, and K. V. Gangadharan, "Design and development of a model free robust controller for active control of dominant flexural modes of vibrations in a smart system," *J. Sound Vibrat.*, vol. 355, pp. 1–18, Oct. 2015.
[32] D. Wu, L. Huang, B. Pan, Y. Wang, and S. Wu, "Experimental study and numerical simulation of active vibration control of a highly flexible beam using piezoelectric intelligent material," *Aerosp. Sci. Technol.*, vol. 37, pp. 10–19, Aug. 2014.
[33] M. Kant, A. Motsara, and A. P. Parameswaran, "Modeling and control of low frequency dynamics of a smart system," *Indian J. Sci. Technol.*, vol. 9, no. 44, Nov. 2016.
[34] M. Kant and A. P. Parameswaran, "Modeling of low frequency dynamics of a smart system and its state feedback based active control," *Mech. Syst. Signal Process.*, vol. 99, pp. 774–789, Jan. 2018.
[35] E. Omidi and N. Mahmoodi, "Hybrid positive feedback control for active vibration attenuation of flexible structures," *IEEE/ASME Trans. Mechatronics*, vol. 20, no. 4, pp. 1790–1797, Aug. 2015.
[36] Y. K. Yong, A. J. Fleming, and S. O. Moheimani, "A novel piezoelectric strain sensor for simultaneous damping and tracking control of a high-speed nanopositioner," *IEEE/ASME Trans. Mechatronics*, vol. 18, no. 3, pp. 1113–1121, Jun. 2013.
[37] B. Bandyopadhyay, T. C. Manjunath, and M. Umapathy, *Modeling, Control and Implementation of Smart Structures: A FEM-State Space Approach*, vol. 350. Berlin, Germany: Springer, 2007.
[38] Y.-H. Lim, V. V. Varadan, and V. K. Varadan, "Closed loop finite element modeling of active structural damping in the frequency domain," *Smart Mater. Struct.*, vol. 6, no. 2, pp. 161–168, Apr. 1997.
[39] T. Manjunath and B. Bandyopadhyay, "Vibration control of a smart flexible cantilever beam using periodic output feedback control technique," in *Proc. 4th Asian Control Conf.*, Singapore, 2002, pp. 1302–1307.
[40] T. C. Manjunath and B. Bandyopadhyay, "Modeling and fast output sampling feedback control of a smart Timoshenko cantilever beam," *Smart Struct. Syst.*, vol. 1, no. 3, pp. 283–308, Sep. 2005.
[41] X. Bu, L. Ye, Z. Su, and C. Wang, "Active control of a flexible smart beam using a system identification technique based on ARMAX," *Smart Mater. Struct.*, vol. 12, no. 5, pp. 845–850, Oct. 2003.
[42] T. Nestorović, N. Durrani, and M. Trajkov, "Experimental model identification and vibration control of a smart cantilever beam using piezoelectric actuators and sensors," *J. Electroceram.*, vol. 29, no. 1, pp. 42–55, Aug. 2012.
[43] P. Van Overschee and B. De Moor, *Subspace Identification for Linear Systems: Theory-Implementation-Applications*. Berlin, Germany: Springer, 2012.
[44] H. J. Palanthandalam-Madapusi, S. Lacy, J. B. Hoagg, and D. S. Bernstein, "Subspace-based identification for linear and nonlinear systems," in *Proc., Amer. Control Conf.*, 2005, pp. 2320–2334.
[45] R. M. Digilov and H. Abramovich, "Flexural vibration test of a beam elastically restrained at one end: A new approach for Young's modulus determination," *Adv. Mater. Sci. Eng.*, vol. 2013, pp. 1–6, Jan. 2013.
[46] C. M. A. Vasques and J. Dias Rodrigues, "Active vibration control of smart piezoelectric beams: Comparison of classical and optimal feedback control strategies," *Comput. Struct.*, vol. 84, nos. 22–23, pp. 1402–1414, Sep. 2006.
[47] X. Dong, Z. Peng, L. Ye, H. Hua, and G. Meng, "Performance evaluation of vibration controller for piezoelectric smart structures in finite element environment," *J. Vibrat. Control*, vol. 20, no. 14, pp. 2146–2161, Oct. 2014.
[48] Q. Liu, J. Gross, S. Pfeiffer, and H. Werner, "A local approach for the LPV identification of an actuated beam using piezoelectric actuators and sensors," *Mechatronics*, vol. 24, no. 4, pp. 289–297, Jun. 2014.
[49] H. Abramovich and B. Pletner, "Actuation and sensing of piezolaminated sandwich type structures," *Composite Struct.*, vol. 38, nos. 1–4, pp. 17–27, May 1997.
[50] R. L. Wang, H. Gu, and G. Song, "Adaptive robust sliding mode vibration control of a flexible beam using piezoceramic sensor and actuator: An experimental study," *Math. Problems Eng.*, vol. 2014, pp. 1–9, 2014.
[51] K. J. Åström and R. M. Murray, *Feedback Systems: An Introduction for Scientists and Engineers*. Princeton, NJ, USA: Princeton Univ. Press, 2021.

ARUN P. PARAMESWARAN received the B.E. degree (Hons.) in electrical and electronics engineering from the College of Engineering Farmagudi, Goa University, in 2006, the M.Tech. degree from MIT Manipal, in 2008, and the Ph.D. degree in system dynamics and control from NITK Surathkal, in 2015. He is currently an Associate Professor with the Department of Electrical and Electronics Engineering, Manipal Institute of Technology (MIT Manipal), Karnataka, India. His current research interests include system design, vibration and its active control, smart materials and their application in vibration control, analysis and control of various low-frequency dynamics, and dynamics of biomedical devices and rehabilitation.

ANJAN N. PADMASALI received the B.Tech. degree in electrical and electronics engineering from the National Institute of Technology Karnataka (NITK), Surathkal, in 2013, and the M.Tech. and Ph.D. degrees in reliability and lighting science from the Manipal Institute of Technology (MIT Manipal), Karnataka, in 2015 and 2020, respectively. He is currently an Associate Professor with the Department of Electrical and Electronics Engineering, Manipal Institute of Technology (MIT Manipal), Karnataka, India. His current research interests include solid-state lighting, reliability studies, and smart materials with their application in measurements and control.

K. V. GANGADHARAN received the B.Tech. degree in mechanical engineering from Calicut University, in 1989, the M.E. degree from the National Institute of Technology (NIT), Trichy, in 1992, and the Ph.D. degree in railroad vehicle dynamics from the Indian Institute of Technology (IIT) Madras, in 2001. He is currently a Professor with the Department of Mechanical Engineering, the Head of the Centre for System Design, and the President of the Institute Innovation Council, National Institute of Technology Karnataka, Surathkal (NITK Surathkal), India. He has a cumulative teaching and research of over 27 years and industrial experience of about one year. He is actively engaged in industrial consultancy and sponsored research projects with more than 120 research publications to his credit. He has filed seven patents with four of them being in the area of medical devices and the remaining three in the area of smart material application. His current research interests include system design, vibration, and its control, smart materials and their applications, structural health monitoring, and product design. He is also actively engaged in creating learning materials for experiential learning of basic concepts in engineering.